$TlCu_{1.73}Fe_{0.27}Se_2$ studied by means of Mössbauer spectroscopy and SQUID magnetometry

2006 J. Phys.: Condens. Matter 18 7373

(http://iopscience.iop.org/0953-8984/18/31/029)

INSTITUTE OF PHYSICS PUBLISHING JOURNAL OF PHYSICS: CONDENSED MATTER

J. Phys.: Condens. Matter **18** (2006) 7373–7382 doi:10.1088/0953-8984/18/31/029

$TlCu_{1.73}Fe_{0.27}Se_2$ studied by means of Mössbauer spectroscopy and SQUID magnetometry

S Kamali-M[1], T Ericsson[1], L Häggström[1], R Berger[2], S Ronneteg[2] and S Felton[3,4]

[1] Department of Physics, Uppsala University, Box 530, SE-751 21 Uppsala, Sweden
[2] Department of Materials Chemistry, Uppsala University, Box 538, SE-751 21 Uppsala, Sweden
[3] Department of Engineering Sciences, Uppsala University, Box 534, SE-751 21 Uppsala, Sweden

E-mail: Lennart.Haggstrom@fysik.uu.se

Received 26 January 2006, in final form 19 June 2006
Published 21 July 2006
Online at stacks.iop.org/JPhysCM/18/7373

Abstract

$TlCu_{2-x}Fe_xSe_2$ is a p-type metal for $x < 0.5$ which crystallizes in a body-centred tetragonal structure. The metal atoms are situated in ab-planes, ∼7 Å apart, while the metal–metal distance within the plane is ∼2.75 Å. Due to the large difference in cation distances, the solid solutions show magnetic properties of mainly two-dimensional character. The SQUID measurements performed for $x = 0.27$ give the c-axis as the easy axis of magnetization, but also show clear hysteresis effects at 10 K, indicating a partly ferromagnetic coupling. The magnetic ordering temperature T_c is 55(5) K as found from both SQUID and Mössbauer spectra. At $T \ll T_c$ the magnetic hyperfine fields are distributed with a maximum at about 30 T, which are compared to the measured magnetic moment per iron atom, which is 0.97 μ_B/Fe as found from SQUID measurements. The experimental results are compared to results using other methods on isostructural Tl selenides.

(Some figures in this article are in colour only in the electronic version)

1. Introduction

As has been shown previously, the ternary copper chalcogenides $TlCu_2X_2$ (X = S, Se, Te) are all metallic conductors [1–3]. The reason, as suggested from various transport measurements in the sulfur and selenium cases [2, 3], is the presence of an electron hole per formula unit at the top of the valence band (VB) due to Se–Se bonding and the fact that copper is monovalent. Consequently, these compounds show only temperature-independent Pauli paramagnetism (PM). The electron band structure was investigated indirectly by x-ray photoelectron spectroscopy [4] and theoretical calculations [5, 6], confirming this view.

[4] Present address: Department of Physics, University of Warwick, Coventry CV4 7AL, UK.

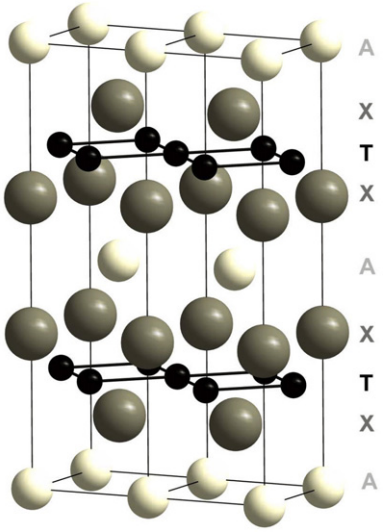

Figure 1. The tetragonal crystal structure of $TlCu_{2-x}Fe_xSe_2$, where A and X stand for Tl and Se, respectively, and T for Cu or Fe. Two unit cells are shown.

Substitution on the transition metal site offers the possibility of changing the physical properties. By introducing other metals (Me) such as gallium or iron for copper, a semiconductor is obtained at the composition $TlCu_{1.5}Me_{0.5}Se_2$, suggesting that two extra electrons (from Me^{3+} instead of Cu^{+}) are simultaneously donated, eventually filling up the valence band [1, 7]. Iron carries at the same time a magnetic moment from its 3d electrons, and interesting magnetic properties are introduced, extensively probed by a battery of experimental methods [7]. Thus, Berger and van Bruggen were able to show how the magnetic properties vary with the degree of substitution in $TlCu_{2-x}Fe_xSe_2$. The paramagnetic iron moments may order below a critical temperature: mainly ferromagnetic (FM) ordering occurs up to $x \sim 0.4$, but near the critical total band-filling value of $x = 0.5$, the solid solution shows a ferrimagnetic character, since the asymptotic paramagnetic temperature suddenly becomes negative. In the metallic range, $0 < x < 0.5$, the Curie temperature of these phases showed a maximum near 80 K for $x \sim 0.4$. At the same time, the variation of magnetic moment, as inferred from saturation measurements, had a maximum near 3 μ_B/Fe (i.e. more than in metallic iron) for $x \sim 0.3$. These effects were interpreted as being due to polarization of the conducting electrons (RKKY type) creating ferromagnetic ordering for low x-values. The increased probability for indirect Fe–Fe coupling for larger x-values makes antiferromagnetic interactions come into play (superexchange) which lower the net moment.

Recently, renewed magnetic measurements on such solutions [8] very nicely confirmed the trend in magnetic moment values, now from single-crystal material at $x = 0.16$ and $x = 0.45$ that gave the extra information that the moments are oriented along the c-axis of the tetragonal cell. The parent compound is of the $ThCr_2Si_2$ structure type (figure 1) where the transition metal atoms are confined to sheets in the ab-plane, with a large sheet separation (roughly 7 Å). Thus, the iron atoms mainly interact within the sheets where they occur with a square sub-lattice arrangement.

In order to probe the iron interactions in this kind of structure, ^{57}Fe Mössbauer spectroscopy has been addressed previously mainly for cases with larger iron contents, such as $TlCuFeSe_2$ [7] or $TlFe_{1.7}Se_2$ [9], the latter with metal vacancies. Within the framework of

a renewed interest in two-dimensional magnetism it was decided to try this method anew, now for compounds with $x \sim 0.3$, a concentration where a large moment was found for the solid solution $TlCu_{2-x}Fe_xSe_2$ [7].

2. Experimental details

2.1. Synthesis and phase characterization

Crystals of nominal composition $x = 0.3$ (with an ^{57}Fe abundance of 33%) were synthesized by mixing stoichiometric amounts of TlSe (presynthesized), Se, Fe and Cu and heating in an evacuated silica tube, followed by controlled slow cooling to allow for nucleation and growth of large crystals. Highly textured crystal material could be obtained in this manner, and the cell parameters were determined from powdered material by x-ray powder diffraction, using a Guinier–Hägg camera equipped with strictly monochromatic Cu $K\alpha_1$ radiation. Germanium was used for calibration. The cell axes were found to be $a = 3.9175(3)$ Å and $c = 13.864(2)$ Å which, according to the Vegard's law calibration curve [7], translates into $x = 0.27$.

2.2. Magnetometry

For the measurements by a SQUID (superconducting quantum interference device) magnetometer (MPMS XL), single-crystal material with a mass of 23.5 mg was stacked with a common $\langle 001 \rangle$ orientation (normal to the flat surface habitus). Thereby it was possible to get data from two principal orientations, either perpendicular to the c-axis or parallel to it, important for the analysis when remembering that the spin-carrying species (iron) is strictly confined to the ab-plane.

The magnetic behaviour as a function of temperature was probed in two manners: recording data on heating, either after applying the field after cooling (zero field cooling, zfc), or applying the field already during the cooling step (field cooling, fc). In both cases, the applied field was 100 Oe. The field dependence of the magnetization was investigated by changing the field while keeping the sample at a constant temperature.

2.3. Mössbauer spectroscopy

The absorber was manufactured by grinding the crystals to a fine powder which was then mixed with BN and finally gently pressed into a ring of copper. The absorber thickness was 0.74 mg Fe cm^{-2}. Aluminium foils were glued on both sides of the ring to keep the absorber intact, it being mounted in a He-flow cryostat for low-temperature measurements. The transmission spectrometer was of constant acceleration type using 512 channels for storing data. Two spectra, in forward and backward directions of the same source (Co*Rh* at room temperature), were recorded simultaneously. The spectra recorded in the backward direction were used for calibration with an iron foil at room temperature as absorber. The spectra were folded and analysed using the Mössbauer fitting program 'Recoil' [10].

3. Results

3.1. Magnetometry results

The temperature dependence of the magnetization (expressed as M/H) for a constant field of 100 Oe is given in figure 2. There is a pronounced difference between the two orientations,

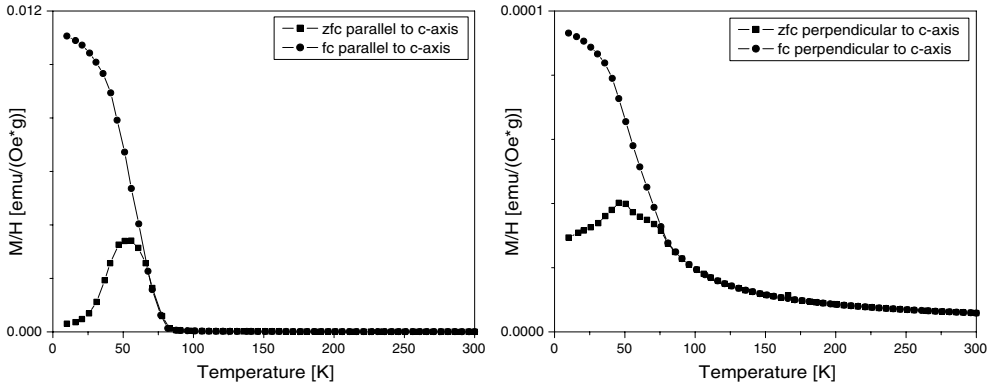

Figure 2. The magnetization versus temperature per applied field and mass in cases that the applied field is in the *c*-direction (left panel) and in the *ab*-plane (right panel). The *y*-scale is very different in the two cases. This indicates that the easy axis is the *c*-axis.

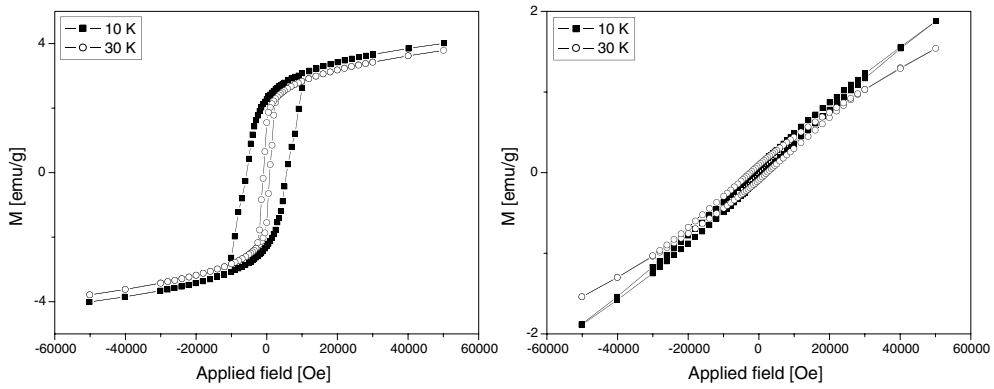

Figure 3. The magnetization as a function of applied field, in the *c*-direction (left panel) and in the *ab*-plane (right panel). Different scales on the *y*-axis are used.

the M/H value being around 100 times higher with the applied field parallel with the *c*-axis compared to perpendicular to it. Both orientations indicate, as best determined from the inflexion of the fc branch, an ordering temperature of about 55 K.

The magnetization data are very different for the two orientations (see figure 3). Considering that the crystal material was not exactly single-crystalline, small deviations from complete alignment are expected. However, a complete saturation is not achieved even for large applied fields. Therefore, a small paramagnetic component is likely present in the hysteresis measurements. The data from the *ab*-plane show correspondingly mainly pure paramagnetic behaviour, only a little marred by a small amount of ferromagnetic behaviour. Therefore, the saturation moment was determined in two steps. First, $M_{\rm sat}\ (T)$ was taken as the intercept on the M-axis for $H = 0$ from a linear extrapolation using high H-values, realizing the symmetry around the origin. Second, the $M_{\rm sat}\ (T)$-values for $T = 10$ and 30 K were extrapolated to $T = 0$ K. By this procedure, $M_{\rm sat}(0) = 3.2$ emu g^{-1} was found. From this, and $x = 0.27$, we obtain an average iron moment of 0.97 $\mu_{\rm B}$/Fe.

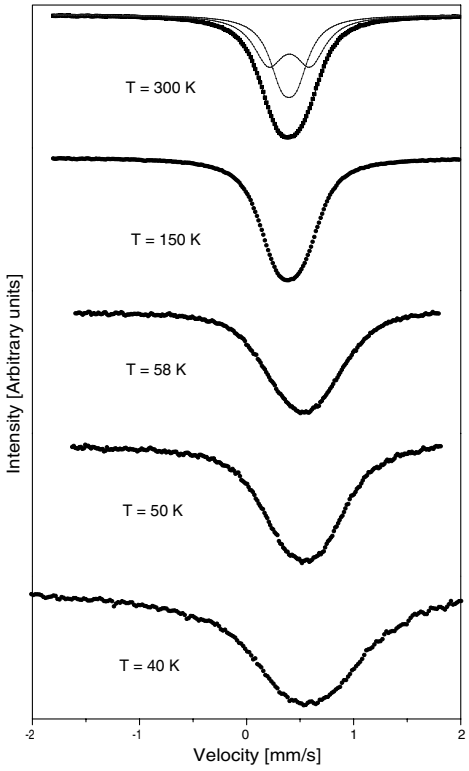

Figure 4. The Mössbauer spectra at 300 K down to 40 K. The absorbances were about 3%.

3.2. Mössbauer spectroscopy and fittings

The Mössbauer spectrum recorded at room temperature (see figure 4) is a symmetrical broad singlet. However, the full width at half maximum, Γ_{exp}, is $\approx$0.56(2) mm s^{-1}, so the Fe atoms do react to hyperfine interactions. The very symmetrical profile indicates approximately the same centre shifts (CSs) for all iron atoms, but a smooth distribution in quadrupole splittings (Δ). The CS is defined as the centre of the resonance lines and is connected to the isomer shift (δ) and second Doppler shift (SOD) via CS $= \delta +$ SOD. Using a two-doublet fit, we obtain CS $=$ 0.40(1) mm s^{-1} with $|\Delta| =$ 0.13(1) and 0.38(1) mm s^{-1}, with $\Gamma_{exp} =$ 0.28(1) and 0.35(1) mm s^{-1}, respectively. The average value found for $|\Delta| =$ 0.27(1) mm s^{-1}.

The spectra recorded between 200 and 50 K show similar bell-shaped profiles. The average quadrupole splitting increases with decreasing temperature to 0.38(1) mm s^{-1} at 50 K. The intensities for the two doublets do not change significantly when decreasing the temperature and are on the average 59(5)% and 41(5)% for the low $|\Delta|$ and high $|\Delta|$ value components, respectively. Γ_{exp} for the profile is plotted in figure 5. The extra broadening starts around 58 K and becomes very significant below 50 K. The spectrum at 30 K shows resolved lines but with obviously very broad distribution in magnetic hyperfine fields. The distribution sharpens up when going to 20 K and is rather narrow at 10 K (figure 6). Assuming a random occupation of the Fe and Cu atoms in the two-dimensional network results in certain coordination probabilities for the Fe atom in this Cu–Fe plane. The nearest neighbour (nn) distance is 2.77 Å (4 atoms) and the next nearest neighbour (nnn) distance is 3.92 Å (4 atoms), while the nnnn and nnnnn distances are 5.55 Å (4 atoms) and 6.19 Å (8 atoms). Here it may

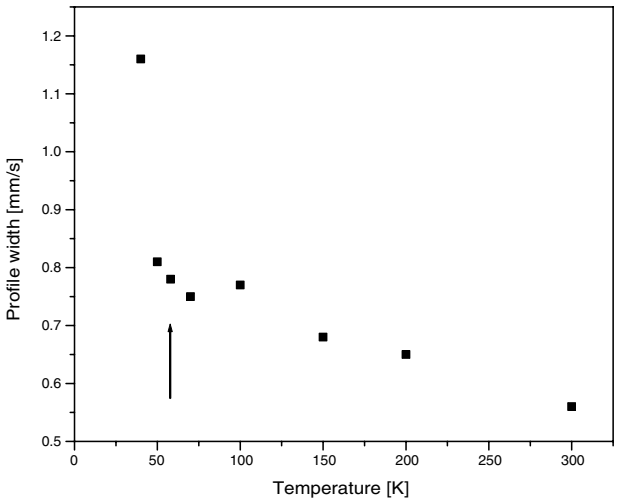

Figure 5. Γ_{exp} of the Mössbauer resonance spectra as a function of temperature. This shows that the transition temperature is about 55 K, as marked by the arrow.

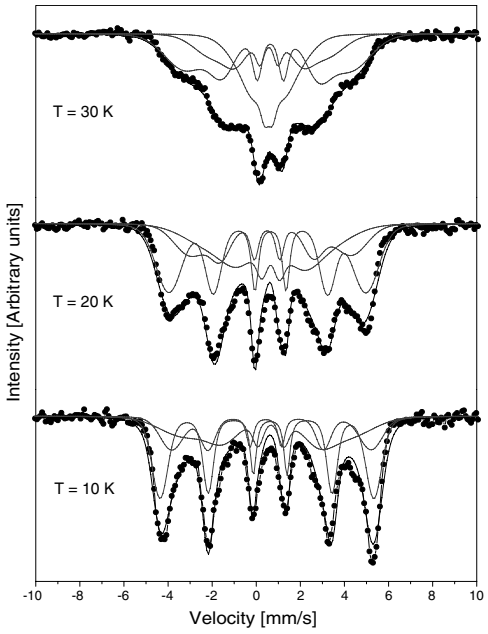

Figure 6. The Mössbauer experimental and fitted spectra for low temperatures, 30, 20 and 10 K. The absorbances were about 1%.

be emphasized that the distance between the Cu–Fe-planes are 6.93 Å in the present case. Restricting to nn and nnn coordination shells gives the occupation probabilities presented in table 1 and figure 7.

It was possible to fit the spectra, recorded at 10 and 20 K, with reasonably good results using only three subpatterns with intensities locked to table 1, row c. The centre shifts were restricted to be same for all subpatterns as also were the Γ_{exp}. The magnetic hyperfine field B_{hf}

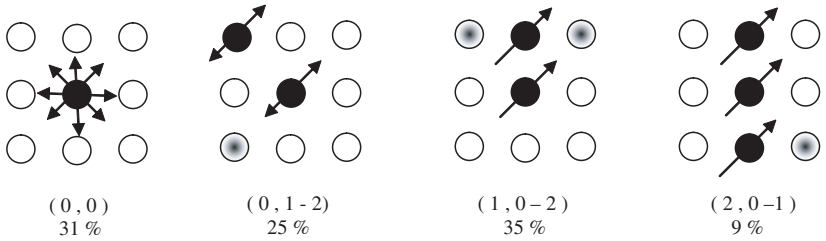

Figure 7. Different Fe coordination possibilities viewed in projection of the Cu–Fe quadratic *ab*-plane along the crystal [001] direction. Filled and unfilled circles indicate Fe and Cu atoms, respectively, while half-filled circles indicate that the position is occupied either by a Cu or an Fe atom. The coordinations depicted are, from left to right, $(x, y) = (0, 0)$, (0, 1–2), (1, 0–2) and (2, 0–1), where (x, y) stands for x Fe atoms as nn and y Fe atoms as nnn. The coordination probabilities are, from left to right, 31%, 25%, 35% and 9%. The Fe magnetic moment fluctuations are schematically drawn in accordance with the findings from the fitting of the Mössbauer spectra (see below). The fluctuation frequencies decrease for increasing number of Fe as nn and nnn.

Table 1. Coordination probabilities for an Fe atom in the *ab*-plane network assuming random occupation of Cu and Fe atoms. Here (x, y) stands for x Fe atoms as nn and y Fe atoms as nnn. The probabilities have been merged into five coordinations in row (b) and into three in row (c).

Coordination (x, y)	(0, 0)	(0, 1)	(0, 2)	(1, 0)	(1, 1)	(1, 2)	(2, 0)	(2, 1)	(3, 0)
(a) Probabilities (%)	31	20	5	20	12	3	5	3	1
(b) Probabilities (%)	31	25		20	15			9	
(c) Probabilities (%)	31	25				44			

Table 2. The magnetic hyperfine field B_{hf} and the Gaussian distribution σ, centroid shift CS, and quadrupole shift ϵ of the different spectral components at low temperatures. Intensities were constrained to 44%, 25% and 31% for the spectral components 1, 2 and 3 respectively. Estimated errors in B_{hf} and σ are ± 0.5 T, in CS $\pm$ 0.01 mm s^{-1} and in $2\epsilon \pm 0.05$ mm s^{-1}. The individual Lorentzian linewidth was the same for all lines, 0.29 mm s^{-1}.

Temp. (K)	CS (mm s^{-1})	B_{hf1} (T)	σ_1 (T)	$2\epsilon_1$ (mm s^{-1})	B_{hf2} (T)	σ_2 (T)	$2\epsilon_2$ (mm s^{-1})	B_{hf3} (T)	σ_3 (T)	$2\epsilon_3$ (mm s^{-1})
30	0.58	23.2	5.4	−0.12	15.9	4.8	0.02	6.7	4.4	0.05
20	0.58	27.7	3.3	−0.14	22.6	4.2	0.16	15.0	7.4	−0.16
10	0.57	30.1	1.8	−0.14	28.1	2.8	0.25	22.3	6.7	−0.21

and its Gaussian distribution σ and the electric quadrupole shift parameter ϵ were, however, free to vary for each subpattern in the fitting. The spectra and the fittings are shown in figure 6 and the obtained parameter values are given in table 2. The spectrum at 30 K was also fitted by the same model, although here the hyperfine field distributions became very large (table 2).

4. Discussion

Felton *et al* [8], using the SQUID technique, measured a saturation moment of 1.5 μ_B/Fe for $x = 0.16$ and 0.66 μ_B/Fe for $x = 0.45$ in $TlCu_{1-x}Fe_xSe_2$. We measure here, using the same technique, 0.97 μ_B/Fe for $x = 0.27$. A linear interpolation, using Felton's values, gives 1.18 μ_B/Fe for $x = 0.27$, thus in reasonable agreement with our result and the VB model presented in [7]. Felton *et al* found $T_c = 65$ K for $x = 0.16$ and two transitions at about 70 and 130 K (weak) for $x = 0.45$. We obtained here $T_c = 55(5)$ K for $x = 0.27$ and no tendency to

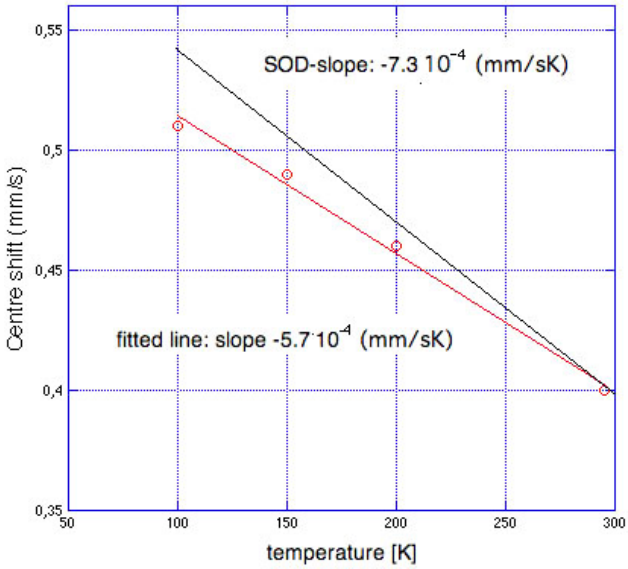

Figure 8. The centre shift (CS) as a function of temperature. For comparison the SOD function is also included.

transition above 100 K. Our results then agree with Felton's lower transition temperature. The mentioned transition at 130 K may come from the Verwey transition in magnetite, it being an impurity too minor to be detected by XRD. Berger and van Bruggen also got minor amounts of magnetite in their samples [7]. Furthermore, the easy axis of magnetization has got to be parallel with the c-axis for $x = 0.27$, as was also found earlier for $x = 0.16$ and 0.45 [8]. The magnetic coupling then seems to be of the same type in the whole region $x < 0.5$, where $TlCu_{2-x}Fe_xSe_2$ is a p-type metal. Also the isostructural non-stoichiometric phase $TlFe_{2-y}Se_2$, with $y \approx 0.3$–0.4, does have the easy magnetization in the c-axis direction [9, 11], while the magnetic moments form a helix in the ab-plane in $TlCo_2Se_2$ [12].

The centre shift increases with decreasing temperature (figure 8). However, the high-temperature linear slope is -6×10^{-4} mm/(sK), thus somewhat less steep than the second order Dopplershift (SOD) high-temperature variation, it being -7.3×10^{-4} mm/(sK). One cause for the difference could be the volume contraction at lowering temperatures, squeezing more Fe s-electrons into the nuclear volume. However, if it had been mainly Fe 3d-electrons which had been compressed, then the CS should have increased instead at lowering temperatures as a result of shielding effects. In $TlFe_{1.7}Se_2$ the slope is -6.7×10^{-4} mm/(sK) in the temperature interval 100–458 K [11] and -7.3×10^{-4} mm/(sK) for $TlFe_{1.6}Se_2$ in the interval 100–438 K as an average value for three Mössbauer patterns [9]. As these isostructural Tl selenides show normal CS(T)-values, we assume that the deviation from normal SOD-shift behaviour for $TlCu_{1.73}Fe_{0.27}Se_2$ is not due to volume contraction at lowering temperatures. It might be due to a temperature-dependent transfer of electrons from Fe to Se instead.

The centre shift obtained for $TlCu_{1.73}Fe_{0.27}Se_2$ at room temperature, 0.40 mm s^{-1}, is quite low compared to 0.57 mm s^{-1} as obtained for $TlCuFeSe_2$ [13]. The result may be understood using the previously mentioned VB model [7]: the Se 4p-band is filled in $TlCu_{2-x}Fe_xSe_2$ for $x = 0.5$. For higher x-values there is a back-donation of electrons to iron, resulting in an increased CS (increased ferrous character, probably complete at $x = 1$). The CSs at room temperature in other related structures are 0.51 mm s^{-1} (average value) in $TlFe_{1.6}Se_2$ [9],

0.55 mm s^{-1} in $TlFe_{1.7}Se_2$ [11] and 0.49 mm s^{-1} in $TlCo_2Se_2$ doped with 2% ^{57}Fe [12]. The result for the two former examples is in line with the model: both should have a filled Se 4p VB and the ferrous character should be higher in the '$Fe_{1.7}$' case compared to the '$Fe_{1.6}$' case, while the situation in the Co case is unclear. Unfortunately, the full solid solution series $TlCu_{2-x}Fe_xSe_2$ has not been studied by Mössbauer spectroscopy as a function of x, due to experimental difficulties (high atomic absorption of the 14.4 keV γ-radiation by Tl and Se, making doping by ^{57}Fe necessary).

A random distribution of iron atoms over the metal sites gives the Fe coordination probabilities presented in table 1. Fe will be surrounded by four Cu atoms as nn in 56% of the cases and by three Cu and one Fe in 35%. Other configurations (two and more Fe in the nearest metal shell) will only cover 9% of the cases. Assuming a more regular Fe surrounding having the lower $|\Delta|$, we can correlate 'four Cu'-surroundings to the smaller $|\Delta|$-values, while 'Fe-neighbours' give higher $|\Delta|$-value. Other atoms as nnn and nnnn etc also influence $|\Delta|$, resulting in the smooth $|\Delta|$-distribution. Such ascriptions do not contradict the experimental intensity values of 59(5)% and 41(5)%, respectively. The low values of $|\Delta|$ in this case are reasonable since the $CuSe_4$ tetrahedron is elongated in the c-direction in $TlCu_2Se_2$, but close to regular in $TlCu_{1.5}Fe_{0.5}Se_2$ [7].

The measured room-temperature electric quadrupole splitting, $|\Delta| = 0.81$ mm s^{-1} in $TlCuFeSe_2$ [7], is higher than obtained here for $TlCu_{1.73}Fe_{0.27}Se_2$ (average value 0.27 mm s^{-1}). This is reasonable as the ferrous character is higher and the $MeSe_4$ tetrahedron is less regular in the former [7]; both factors favour a higher $|\Delta|$.

The low-temperature Mössbauer results indicate that the sharpening of the spectra when going from 30 to 10 K is a result of the local influence on the magnetic hyperfine fields. At 10 K the fields for components 1 and 2 (table 1) are rather close, being 30.1(5) and 28.1(5) T. As assigned component 1 is emanating from Fe atoms having three, two or one Fe atoms as nn, while component 2 is emanating from Fe atoms with no Fe as nn but with one or two Fe atoms as nnn. Component 3, with a field at 10 K of 22.3(5) T and a broad distribution of 6.7 T is emanating from Fe atoms with no Fe atoms as nn or nnn but with one or more Fe atoms in the third or higher coordination shells. These long Fe–Fe distances result in weak magnetic couplings. Consequently the Fe magnetic moments fluctuate with the result of a lower measured magnetic hyperfine field [14] and a broader distribution (figure 7). This explanation is further supported by the result for the 20 and 30 K spectra where the decreased measured fields and even broader Gaussian field distributions are due to increased magnetic moments fluctuation frequencies. The fact that the two spectral components 1 and 2 have a narrow spread in the magnetic hyperfine fields at 10 K means that the Fe moment relaxation times for these coordinations are longer than the Mössbauer time window. Since the observed magnetic hyperfine fields are slightly different (7%) for these two components we can conclude that it is possible to correlate not only the hyperfine parameter $|\Delta|$ (shown above from the analysis of the room-temperature spectrum) but also the hyperfine parameter B_{hf} to the local Fe configurations.

The obtained high-field component at low temperature ($\approx$30 T) is somewhat higher than in non-stoichiometric $TlFe_{1.7}Se_2$ ($B_{hf} = 27.2$ T at 100 K) [11] or $TlFe_{1.6}Se_2$ ($B_{hf} = 27.0$ T at 100 K [9]) and considerably higher than in $TlCo_2Se_2$ ($B_{hf} \leqslant 12$ T in a helical magnetic structure [12]).

5. Conclusion

Mössbauer spectroscopy and SQUID measurements have determined $TlCu_{1.73}Fe_{0.27}Se_2$ to be partly ferromagnetic with the c-axis as the easy axis of magnetization and a T_c of 55(5) K. The saturation moment found, 0.97 μ_B, is lower than previously reported for this compound.

Furthermore, the local probe technique has been able to correlate the local Fe configurations to specific strength of hyperfine interaction parameters. The maximum saturation hyperfine field is high, 30 T, for this rather Fe diluted compound, higher than the isostructural non-stoichiometric $TlFe_{1.7}Se_2$. Further Mössbauer studies of other Cu/Fe ratios are needed in order to reveal the full picture of the system.

References

[1] Brun G, Gardes B, Tédénac J C, Raymond A and Maurin M 1979 *Mater. Res. Bull.* **14** 743
[2] Berger R 1989 *J. Less-Common Met.* **141** 141
[3] Berger R and van Bruggen C F 1984 *J. Less-Common Met.* **99** 113
[4] Karlsson L, Keane M P and Berger R 1990 *J. Less-Common Met.* **166** 353
[5] Vajenine G V and Hoffmann R 1996 *Inorg. Chem.* **35** 451
[6] Shirai M 1995 *Synth. Met.* **71** 1857
[7] Berger R and van Bruggen C F 1985 *J. Less-Common Met.* **113** 291
[8] Felton S, Nordblad P, Ronneteg S and Berger R 2005 *J. Appl. Phys.* **97** 10
[9] Häggström L, Seidel A and Berger R 1991 *J. Magn. Magn. Mater.* **98** 37
[10] Lagarec K and Rancourt D C 1998 *Recoil, Mössbauer Spectral Analysis Software for Windows, version 1.0*
[11] Häggström L, Verma H R, Wäppling R, Bjarman S and Berger R 1986 *J. Solid State Chem.* **63** 401
[12] Kamali S, Häggström L, Ronneteg S and Berger R 2004 *Hyperfine Interact.* **156/157** 315
[13] Häggström L 2006 personal communication
[14] Blum M and Tjon J A 1968 *Phys. Rev.* **165** 446